Iron pnictide superconductivity: from strong coupling point of view

Fu-Chun Zhang, Univ. of Hong Kong

Collaborators:

Wei-Qiang Chen, Univ. Hong Kong
Kai-Yu Yang, ETH-Zurich
Yi Zhou, Univ. Hong Kong/Chinese Univ. of Hong Kong
F Ma and Zhong-Yi Lu, Ren Ming Univ, China

KITP, July 23, 2009

Outline

- **Introduction**
- **Effective Hamiltonian and Pairing Interaction**
- **Pairing symmetry**
- **Iron pnictides and copper oxides**
- **Proposed \pi-junction loop to probe anti-phase s-wave**

Materials

- Discovery: doped LaFeAsO with Tc =26K, Feb. of 2008 (replacing any of 4 elements leads to supercond)
- Highest Tc in pnictides: 56K
- Doped BaFe2As2
- FeSe_x
- …

Layered lattice structure

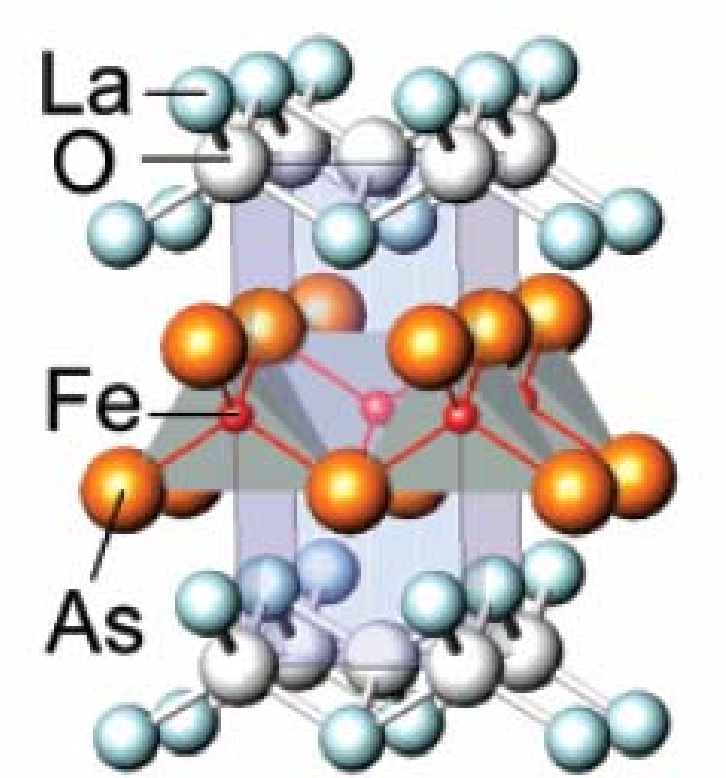

1111

LaFeAsO

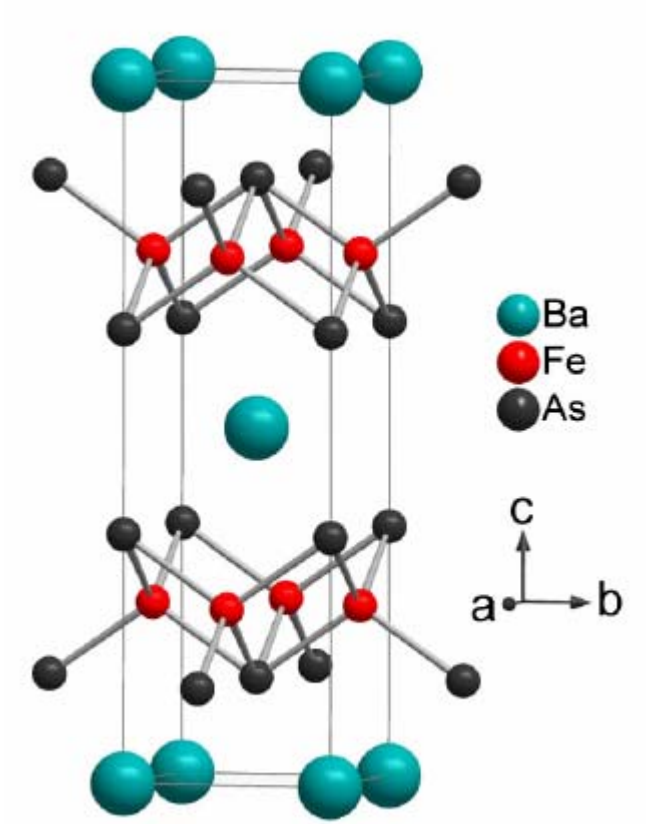

122

BaFe2As2

Parent compound: LaFeAsO

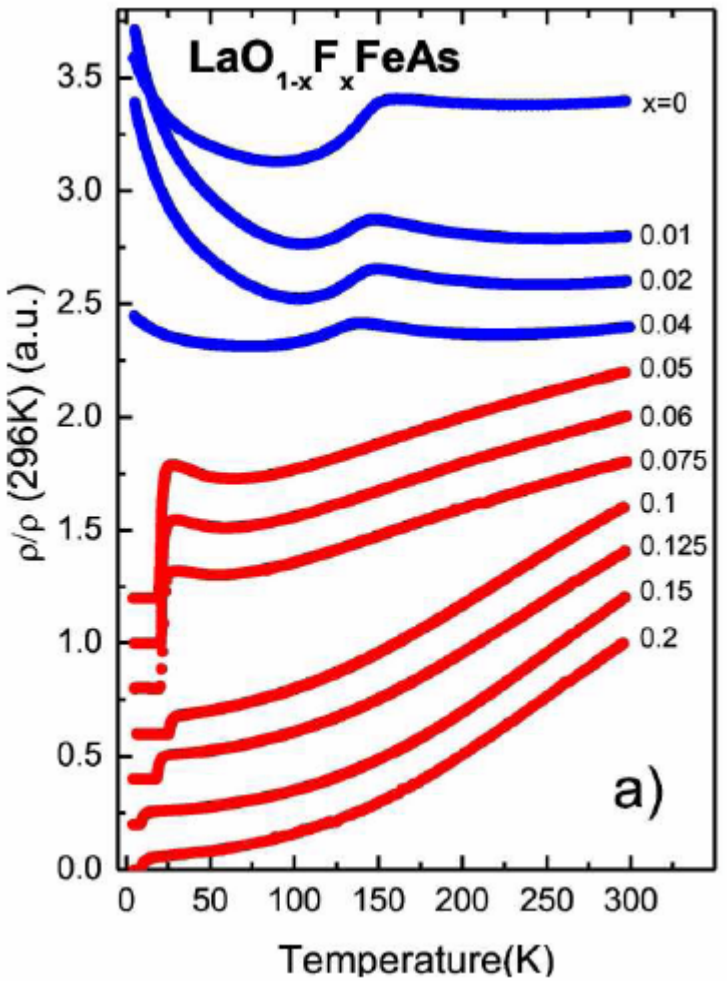

Semimetal, anomaly around 150 K

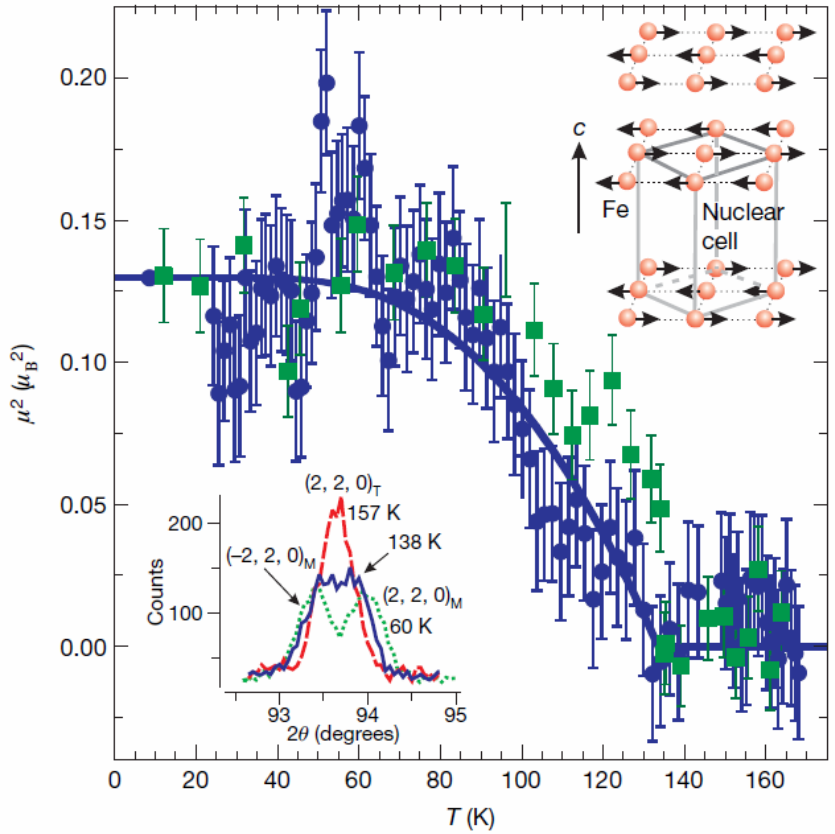

Collinear SDW order (inset)
Moment, M = 0.36(5) μB
T_N = 137 K

Clarina de la Cruz et al. Nature (2008)

Phase diagram with doping

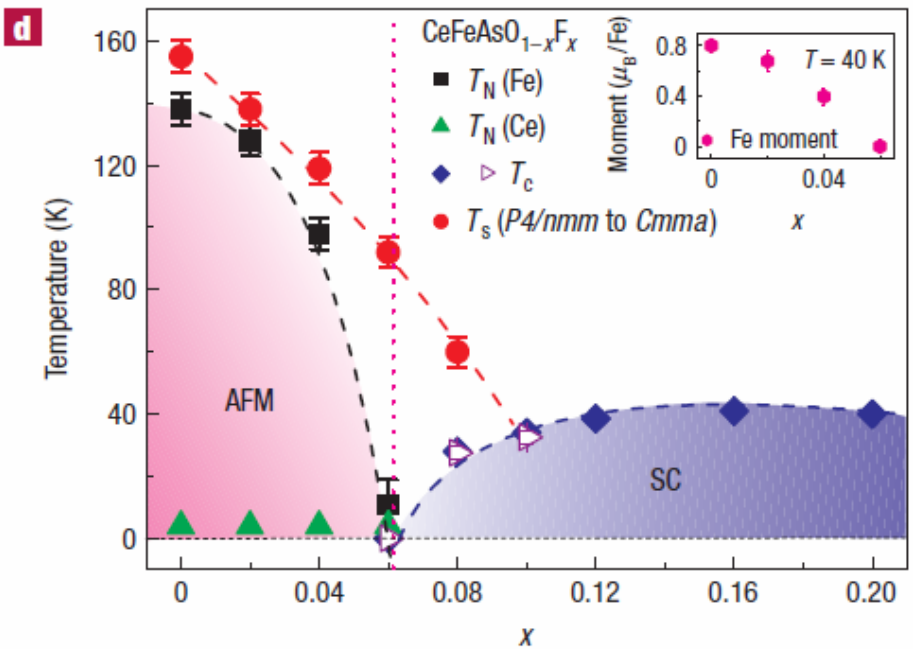

$CeFeAsO_{1-x}F_x$

Jun Zhao et al. Nat. Material (2008)

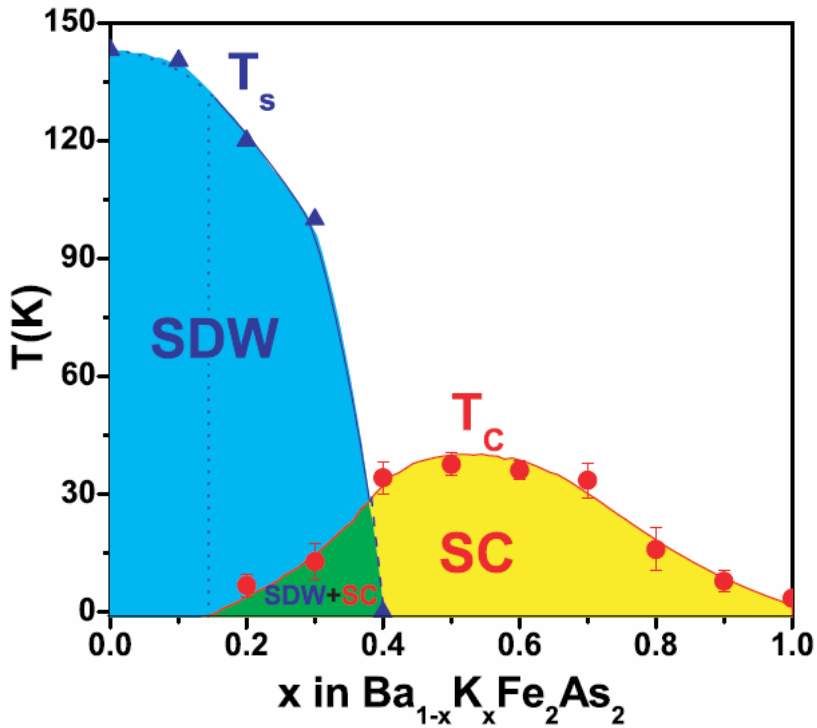

$Ba_{1-x}K_xFe_2As_2$

H. Chen et al. EPL (2009)

possible magnetic origin of SC

- Electron-phonon mechanism unlikely, Boeri, Cohen,..
- Parent compound: SDW below ~130K
- Mag. Moment:~ 0.3 Bohr for 1111,

  ~1 for 122
- Layered structure

Electronic strucuture

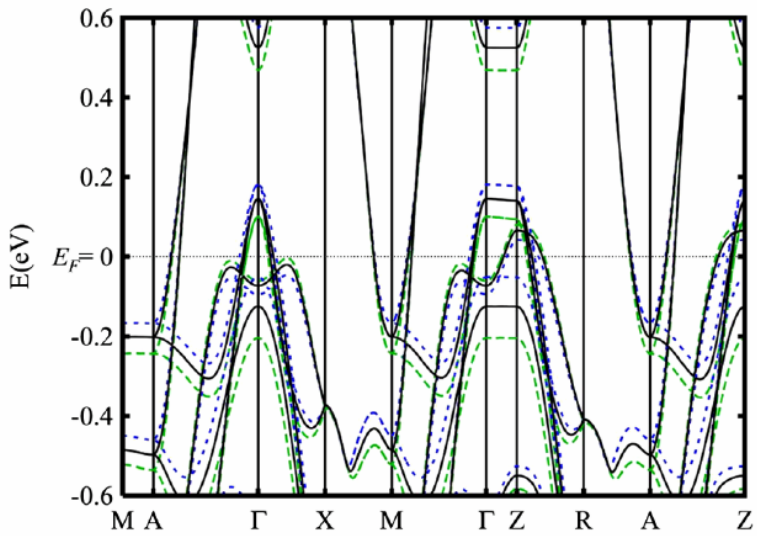

FIG. 2 (color online). Band structure of LaFeAsO around E_F showing the effect of As breathing along z by $\delta z_{\mathrm{As}} = 0.04$ (0.035 Å). The unshifted band structure is indicated by the solid black line, while the shift away (towards) the Fe is indicated by the blue dotted lines (green dashed lines).

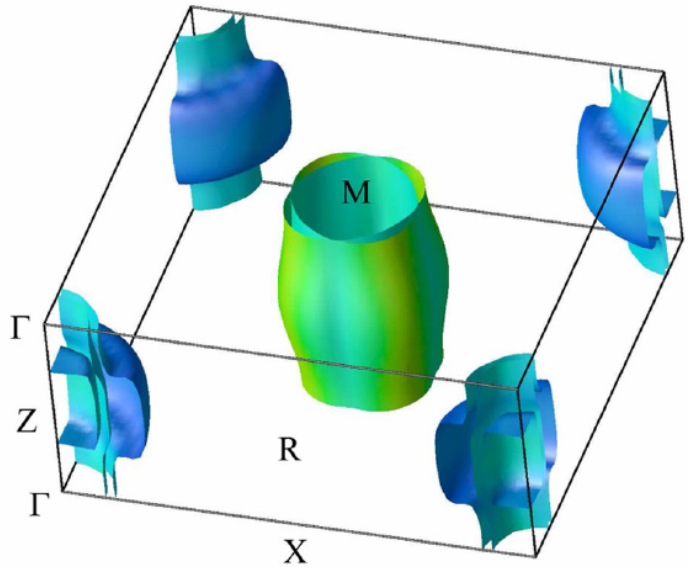

FIG. 3 (color online). LDA Fermi surface of LaFeAsO shaded by velocity [darker (blue) is low velocity]. The symmetry points are $\Gamma = (0, 0, 0)$, $Z = (0, 0, 1/2)$, $X = (1/2, 0, 0)$, $R = (1/2, 0, 1/2)$, $M = (1/2, 1/2, 0)$, $A = (1/2, 1/2, 1/2)$.

Mainly from Fe 3d orbital.

Weak c-axis dispersion.

D. J. Singh and M.-H. Du PRL (2008)

Superconducting state: Nodaless gap

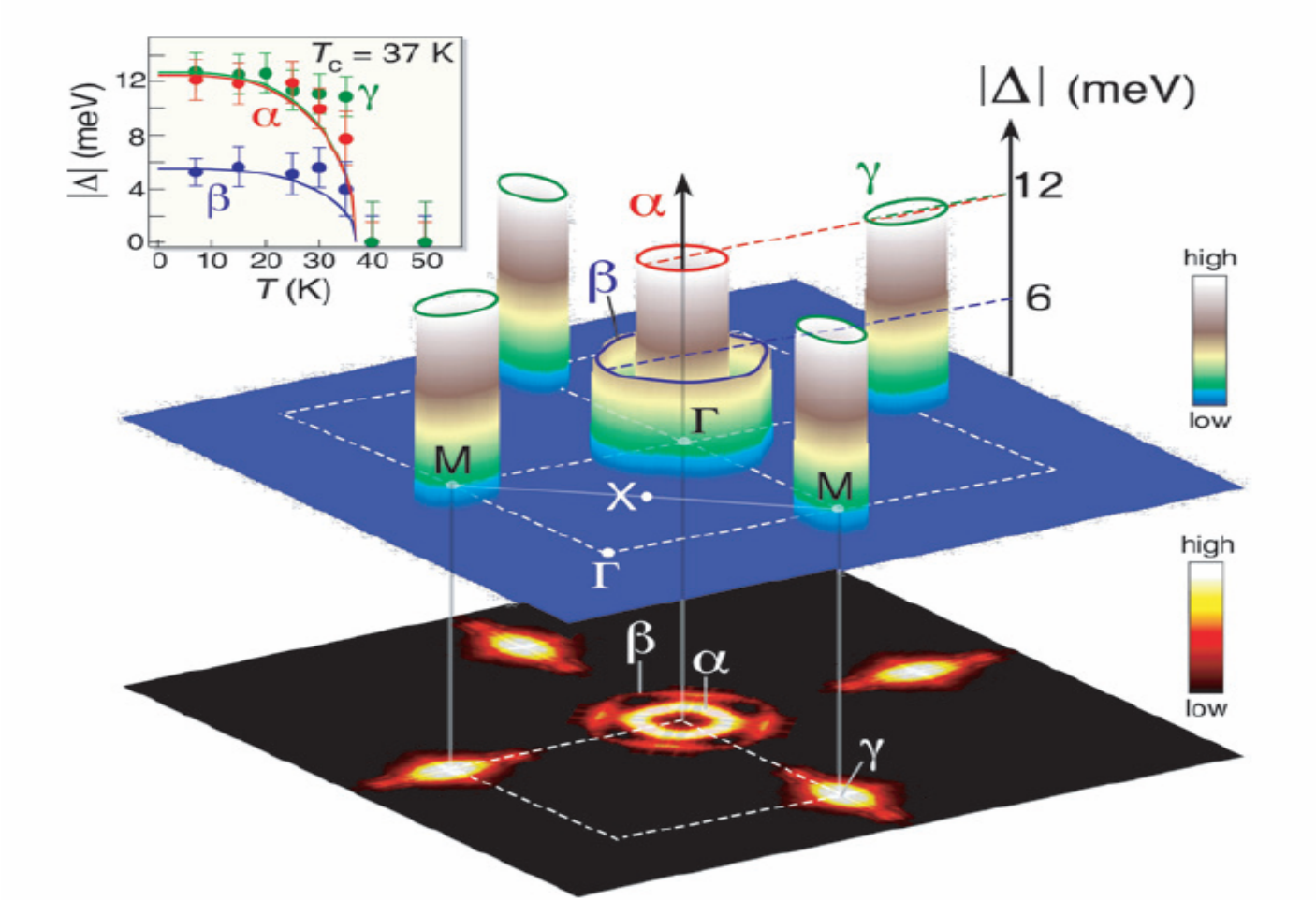

ARPES on $Ba_{0.6}K_{0.4}FeAs$ – by Ding et al, 2008

S-wave universal to all iron-based superconductivity?

penetration depth measurement of Moler et al. on LaOFeP with Tc =6K from scanning SQUID susceptometry indicates nodal superconductivity

Electron correlations in Fe-based compounds – likely moderate

- Parent compound LaFeAsO: AF semi-metal. not a Mott insulator as cuprate, & not a simple metal
- Likely to be near but at the metallic side of Mott insulator metal transition: DMFT of Kotliar et.al.
- Open issue for SDW: FS nesting, J1-J2 model.
- Observed FS similar to LDA, mass renormalized

Likely a system with moderately large correlations

Strong vs weak coupling approaches

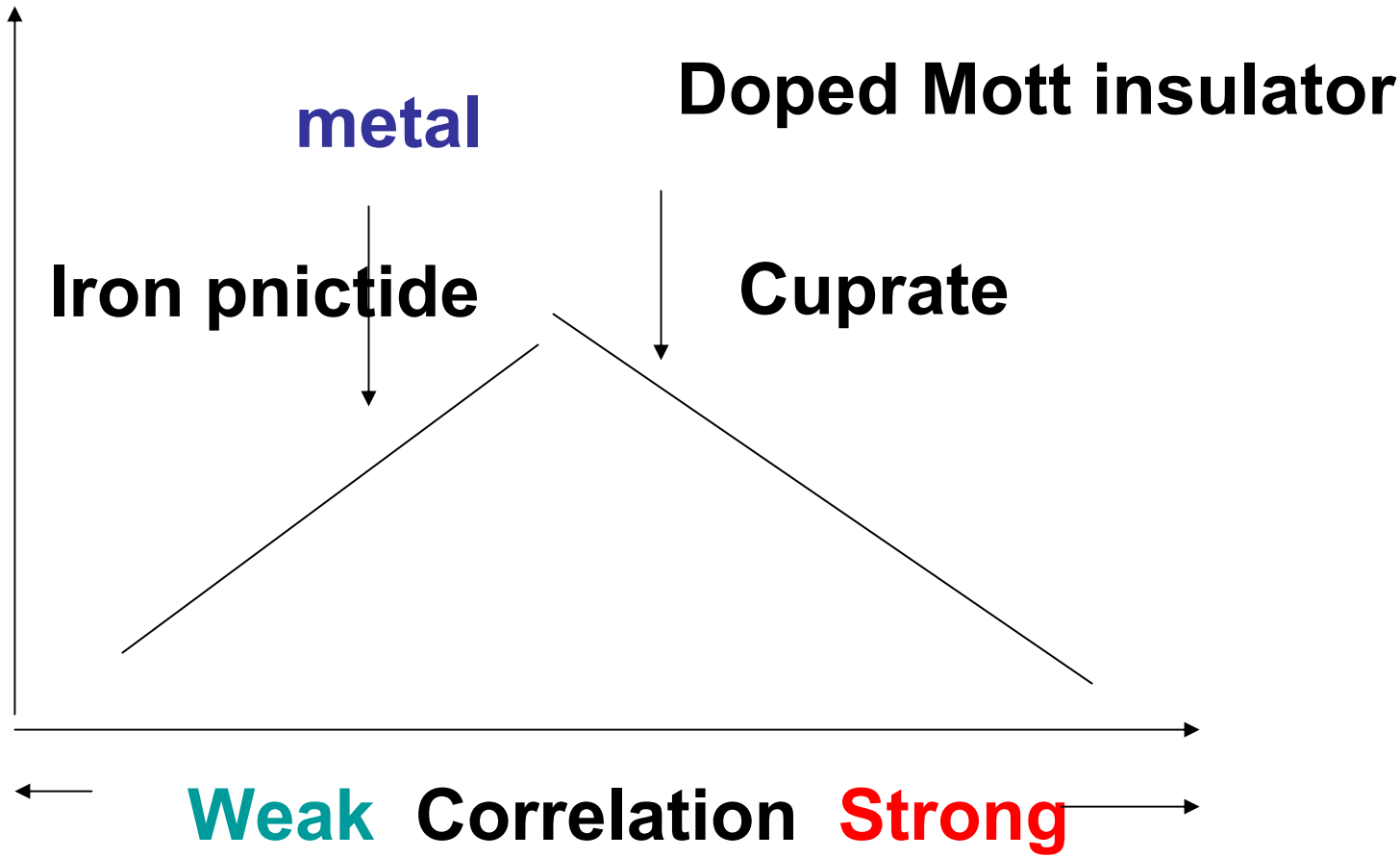

Strong vs weak coupling approaches

- **Cuprate SC**

  strong coupling theory (t-J) for SC and weak coupling functional RG theory give same pairing symmetry

- **Fe-based SC**

1. Weak coupling: fRG (DH Lee), Peter Hirschfeld (next week)
2. Strong coupling approach

--- in this talk, and also Q. Si …

Starting Hamiltonian

- Band structure + on-site Coulomb
- Band structure

  $3d^6$ electrons on Fe-ion. mainly 2 orbitals d_xz and d_yz near Fermi surface

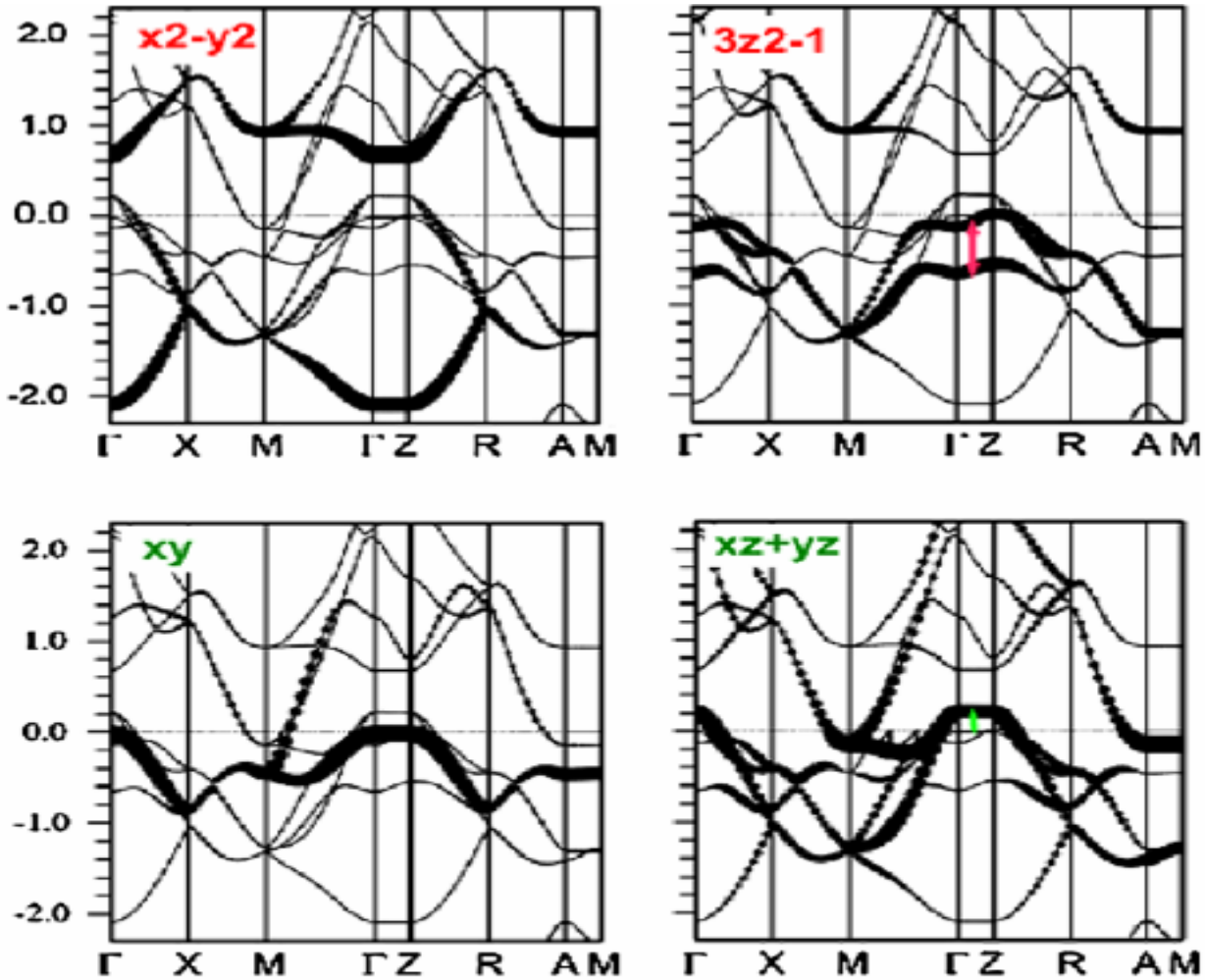

FIG. 2 (color online). Band structure of LaFeAsO, decorated with partial characters of the e_g (top) and t_{2g} (bottom) Fe-d bands. The orientation of the coordinate system is chosen so that Fe-Fe bonds are directed along the x and y axes; the zero of the energy coincides with the Fermi level. The arrows indicate the splitting induced by the elongation/shrinking of the Fe-As tetrahedra (see text).

LAFeASO

LDA, Boeri et al. PRL

Reduced BZ

El doped, Fermi level above 0

dxz, dyz dominant

2-orbital model- tight binding fitting

Tight binding of 2-orbitals, by Raghu et al.
n.n and next n.n hopping

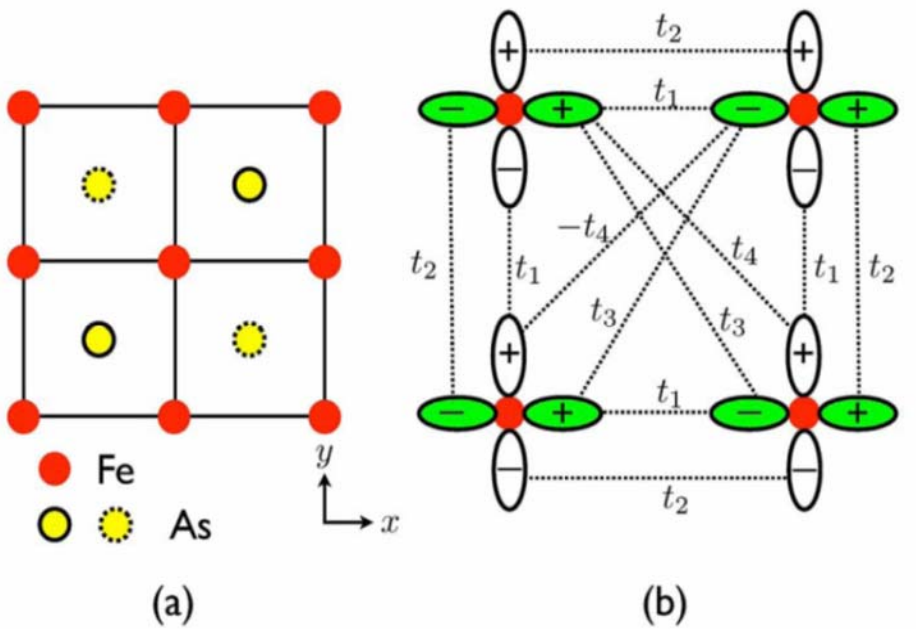

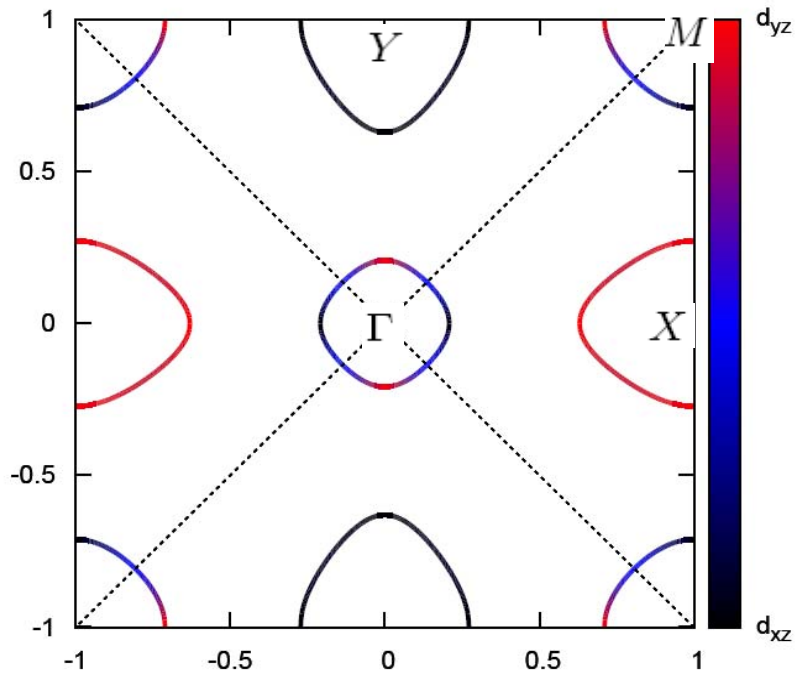

Fermi surface in extended zone, similar to LDA

M-pocket should be 2nd Γ pocket – LDA
In reduced zone, Fermi surface same as LDA

Superconductivity in Fe-based compound

H = H_t + on-site Coulomb term

H_t = tight binding of 2- orbitals

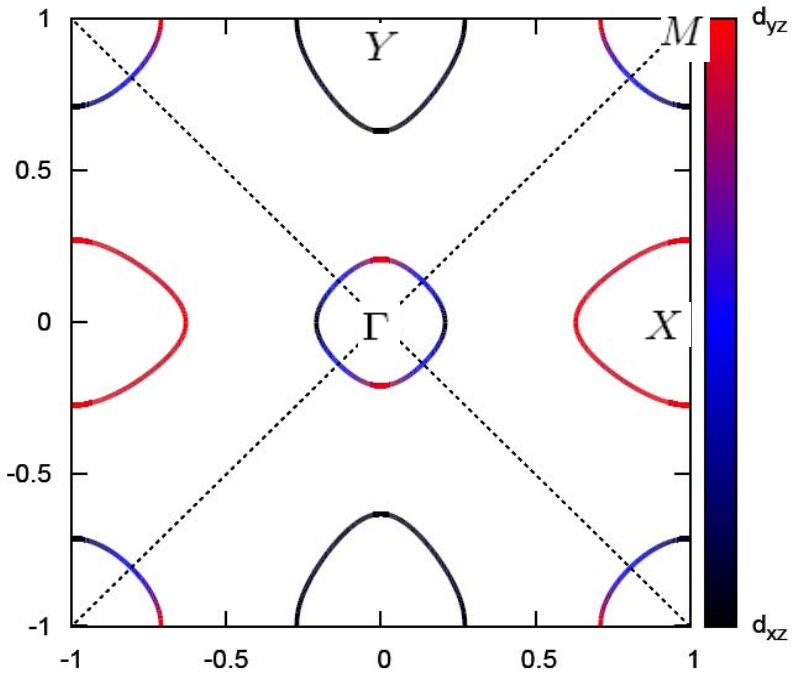

On-site Coulomb interaction

$$H_I = \sum_{i;m=1,2} [U\hat{n}_{im\uparrow}\hat{n}_{im\downarrow} + J\hat{c}^{\dagger}_{im\uparrow}\hat{c}^{\dagger}_{im\downarrow}\hat{c}_{i\overline{m}\downarrow}\hat{c}_{i\overline{m},\uparrow}]$$

$$+ \sum_{i;\sigma\sigma\prime} [U_{12}\hat{n}_{i1\sigma}\hat{n}_{i2\sigma\prime} + J\hat{c}^{\dagger}_{i1\sigma}\hat{c}^{\dagger}_{i2\sigma\prime}\hat{c}_{i1\sigma\prime}\hat{c}_{i2\sigma}]$$

where, U_{12} = U – 2J

2-orbital model for pnictide at large U

- Parent compound: Fe-ions: atomic configuration $3d^6$, two electrons on two orbitals (d_xz, d_yz). Ignore all other orbitals, each ion is "half filled", an insulator compared to semi-metal in expt.
- El-doping: some Fe-ions become $3d^7$, charge carriers.

  $3d^6$ is of two holes and $3d^7$ is spin ½ of a single hole

$3d^6$ 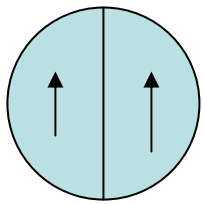 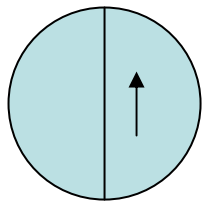 $3d^7$

left half: orbital 1, right half: orbital 2

Doped Fe-compound: spin-1/2 (carrier) with orbital degree of freedom moves in background of two-hole sites.

Large U limit for parent compound

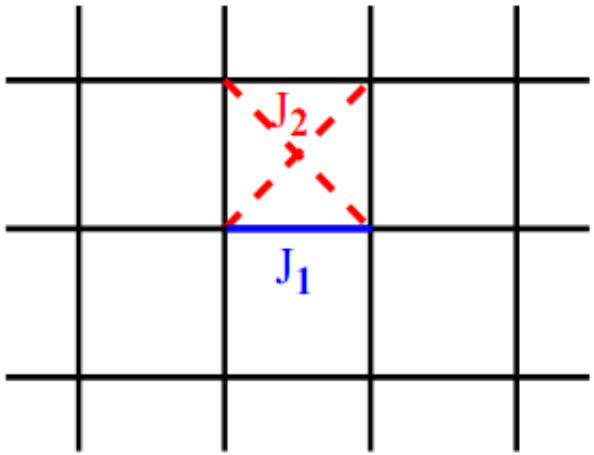

Spin 1 J_1–J_2 model:

$$H_J = \sum_{ij} J_{ij}^{\alpha\beta} \mathbf{s}_{i,\alpha} \cdot \mathbf{s}_{j,\beta} + J_H \sum_{i,\alpha\neq\beta} \mathbf{s}_{i,\alpha} \cdot \mathbf{s}_{i,\beta},$$

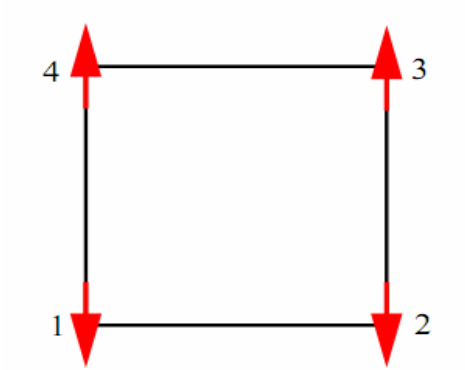

Consistent with SDW results with suitable choice of J's

Collinear magnetic order

Large U limit: el. doped (large J)

$3d^7$ carriers move in a 2-hole background:

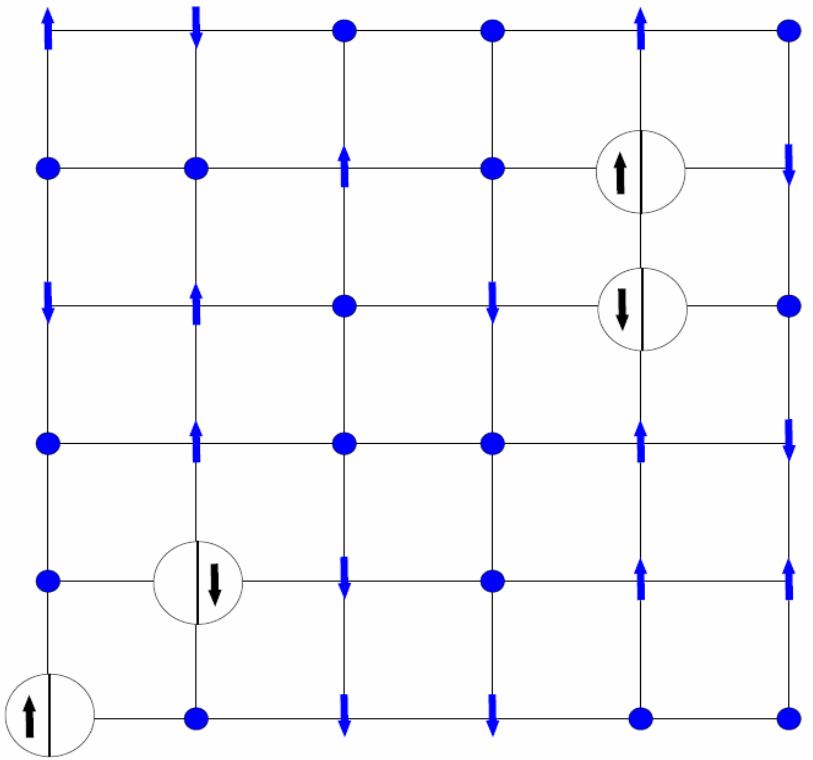

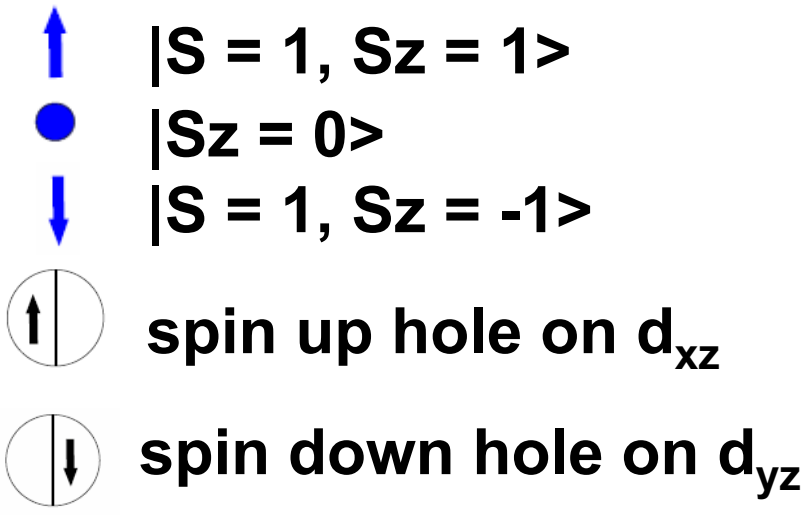

Effective interaction between carriers on neighboring sites i and j

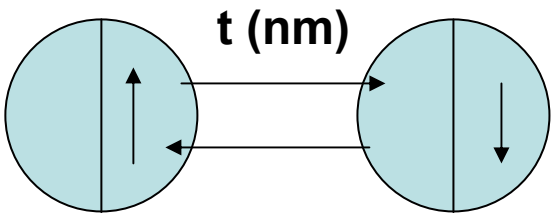

Site i j

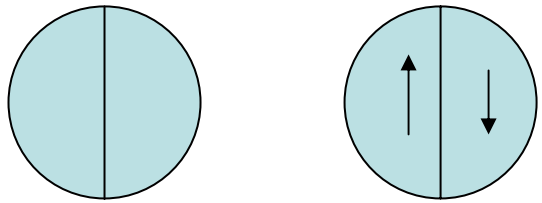

i j

Virtual state, cause energy ~ U

Via virtual hopping process: exchange coupling with orbital degree of freedom

The two $3d^7$ irons can be a spin singlet or a spin triplet

Strong Coupling Theory: Orbital dependent pairings

(n, m : orbital indices 1 or 2) **W. Q. Chen et al. PRL 2009**

$$H_2 = -\sum_{ij}\sum_{nmn'm'}[A_{nm}^{m'n'}(ij)\hat{b}_{nm}^{\dagger}(ij)\hat{b}^{n'm'}(ij)$$ ***Spin-singlet***

$$-\sum_{S_z} B_{nm}^{m'n'}(ij)\hat{T}_{nm}^{S_z\dagger}(ij)\hat{T}_{S_z}^{n'm'}(ij)]$$ ***Spin-triplet***

with $\hat{b}^{nm}(ij) = \frac{1}{\sqrt{2}}(\hat{c}_{in\uparrow}\hat{c}_{jm\downarrow} - \hat{c}_{in\downarrow}\hat{c}_{jm\uparrow})$ *Spin-singlet*

$$A_{nm}^{m'n'}(ij) = [\frac{(-1)^{m+m'}}{U-J} + \frac{1}{U+J}]t_{ij}^{nm}t_{ji}^{m'n'} + \frac{t_{ij}^{n\bar{m}}t_{ji}^{\bar{m}'n'}}{U_{12}+J}$$

$$B_{nm}^{m'n'}(ij) = \frac{(-1)^{m+m'}}{U_{12}-J}t_{ij}^{n\bar{m}}t_{ji}^{\bar{m}'n'}$$

At J/U ~ 1/3, B term large, spin triplet most favored.
We'll focus on singlet here for expt. evidence for singlet

t^{nm} : hopping between orbital n and m, U Coulomb between same orbital, U_{12} between different orbitals, J Hund's coupling

Comparison with exchange interaction in single orbital Hubbard model

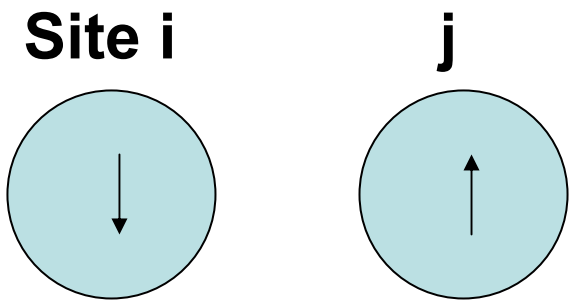

$$H_J = -Jb^{\dagger}(ij)b(ij) = +J(\mathbf{S}_i \cdot \mathbf{S}_j - \frac{1}{4}n_i n_j)$$

$J = \frac{4t^2}{U}$, - J : energy of a singlet pair

Form of effective H for two orbital system Castellani et al.,1979 in study of V_2O_3

$$H_{\mathrm{eff}} = -\sum_{ij}\sum_{nn'm}\sum_{\sigma} t_{ij}^{nm} t_{ij}^{n'm} c_{in\sigma}^{\dagger} c_{in'\sigma} \left(\frac{U_{11}}{U_{11}^2 - J^2}\, n_{jm\,-\sigma} + \frac{U_{12}}{U_{12}^2 - J^2}\, n_{j\,-m\,-\sigma} + \frac{1}{U_{12} - J}\, n_{j\,-m\sigma} \right)$$

$$-\sum_{ij}\sum_{nn'm}\sum_{\sigma} t_{ij}^{nm} t_{ij}^{n'm} c_{in\sigma}^{\dagger} c_{in'\,-\sigma} \left(-\frac{U_{11}}{U_{11}^2 - J^2}\, c_{jm\,-\sigma}^{\dagger} c_{jm\sigma} + \frac{J}{U_{12}^2 - J^2}\, c_{j\,-m\,-\sigma}^{\dagger} c_{j\,-m\sigma} \right)$$

$$-\sum_{ij}\sum_{nn'm}\sum_{\sigma} t_{ij}^{nm} t_{ij}^{n'\,-m} c_{in\sigma}^{\dagger} c_{in'\sigma} \left(-\frac{J}{U_{11}^2 - J^2}\, c_{jm\,-\sigma}^{\dagger} c_{j\,-m\,-\sigma} - \frac{J}{U_{12}^2 - J^2}\, c_{j\,-m\,-\sigma}^{\dagger} c_{jm\,-\sigma} - \frac{1}{U_{12} - J}\, c_{j\,-m\sigma}^{\dagger} c_{jm\sigma} \right)$$

$$-\sum_{ij}\sum_{nn'm}\sum_{\sigma} t_{ij}^{nm} t_{ij}^{n'\,m} c_{in\sigma}^{\dagger} c_{in'\,-\sigma} \left(\frac{J}{U_{11}^2 - J^2}\, c_{jm\,-\sigma}^{\dagger} c_{j\,-m\sigma} - \frac{U_{12}}{U_{12}^2 - J^2}\, c_{j\,-m\,-\sigma}^{\dagger} c_{jm\sigma} \right). \qquad (3.10)$$

Ours identical to this,
but written in the form of paired state

Results on pairing states

Qualitative analyses

Pairing term in k-space

$$H_2 = -A_{nm}^{m'n'}(\mathbf{q}) b_{nm}^{\dagger}(\mathbf{k}) b_{m'n'}(\mathbf{k}')$$

A(**q**) Fourier transform of A(ij).

Much of physics can be understood in diagonal part of b,

$A_n^m = A_{nn}^{mm}$, we have analytical results for pairings.

Pair scatterings: orbital point of view

$$A_{11}(\mathbf{q}) = \frac{4U(t_1^2 \cos q_x + t_2^2 \cos q_y)}{U^2 - J^2} + (\frac{1}{U+J} + \frac{2}{U-J}) 4t_3^2 \cos q_x \cos q_y$$

$$A_{22}(\mathbf{q}) = A_{11}(q_y, q_x)$$

$$A_{12}(\mathbf{q}) = \frac{4}{U+J} t_3^2 \cos q_x \cos q_y - \frac{4J}{U^2 - J^2} t_1 t_2 (\cos q_x + \cos q_y)$$

Different from weak coupling

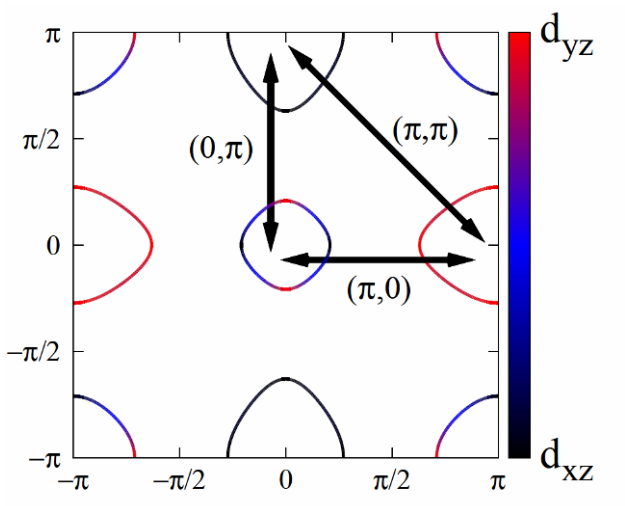

Intra-orbital scattering (A_{11} and A_{22}) stronger than inter-orbital one (A_{12}).

q ~ (0 , 0): A_{11} and A_{22} dominant, both attractive, favor same sign in one pocket

q ~ (0 ,π): A_{11} and A_{22} dominant, both repulsive, favor different sign between electron and hole pockets

q ~ (π,π): A_{12}, positive for small J/U and negative for large J/U

Pair scattering amplitudes (J=0)
negative: attraction

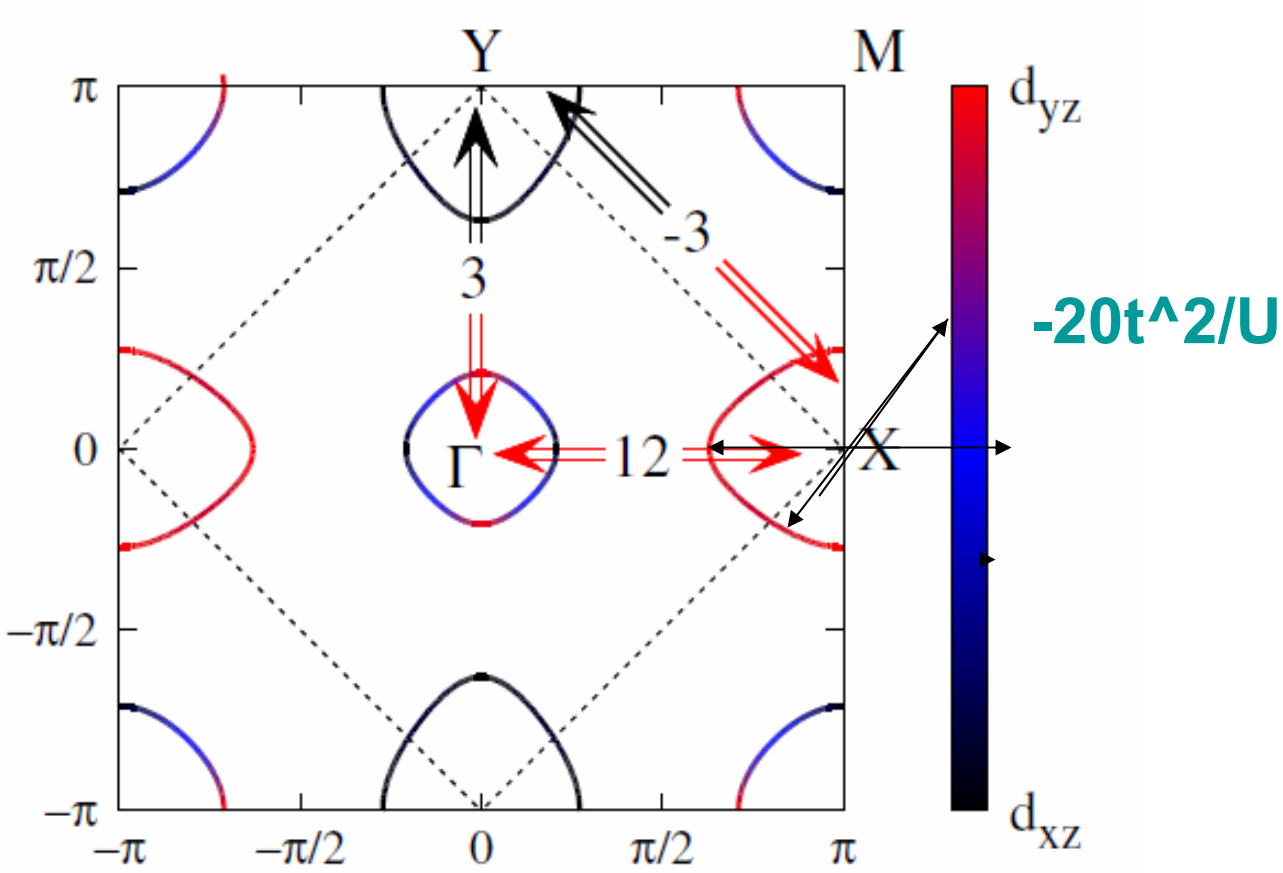

This pairing analysis leads to s- wave with antiphase

Quantitative study

- Gap equations can be solved self-consistently
- Only A_{1g} (s-wave) and B_{1g} (d-wave) states are found to have lower energy

Kinetic term is renormalized by a factor of g_t

Pairing term is renormalized by a factor of g_s.

Below we set $g_t=g_s=1$, effectively renormalize t and U to study the pairing symmetry

Mean field approach

- Mean fields: $\Delta_{nm}(\vec{\tau}) = \frac{1}{2}\left\langle c_{in\uparrow}c_{i+\vec{\tau}m\downarrow} - c_{in\downarrow}c_{i+\vec{\tau}m\uparrow}\right\rangle$
- Independent ones:

$$\Delta_{11}(\hat{x}),\ \Delta_{22}(\hat{x}),\ \Delta_{12}(\hat{x}),\ \Delta_{21}(\hat{x}),\ \Delta_{11}(\hat{x}+\hat{y}),\ \Delta_{12}(\hat{x}+\hat{y})$$

- Mean field Hamiltonian:

$$H_{MF} = \sum_{\mathbf{k}} \hat{\psi}^{\dagger}_{\mathbf{k}} \begin{pmatrix} \xi_{\mathbf{k}} & V(\mathbf{k}) \\ V^{\dagger}(\mathbf{k}) & -\xi_{\mathbf{k}} \end{pmatrix} \hat{\psi}_{\mathbf{k}},$$

$$V_{\alpha\beta}(\mathbf{k}) = \sum_{nmm'n';\tau} A^{m'n'}_{nm}(\vec{\tau})\Delta^{*}_{nm}(\vec{\tau})e^{i\mathbf{k}\cdot\vec{\tau}}u_{m'\alpha}(\mathbf{k})u_{n'\beta}(\mathbf{k})$$

--- Pairing amplitude

u's : matrix between band and orbital

- Quasiparticle energy $E_{\pm}(\mathbf{k}) = \sqrt{w_{+}^{2} + V_{+-}^{2} \pm \sqrt{w_{-}^{4} + V_{+-}^{2}[(\delta\xi)^{2} + 4\bar{V}^{2}]}}$

w and all other symbols are related to V and ξ

According to symmetry analysis:

$$V(\mathbf{k}) = V^0(\mathbf{k})\sigma_0 + V^1(\mathbf{k})\sigma_1 + V^3(\mathbf{k})\sigma_3.$$

For A1g symmetry:

$$\begin{aligned}
V^0(\mathbf{k}) &= \frac{4(\cos k_x + \cos k_y)}{U^2 - J^2}\Big[t_1(t_1U - t_2J)\Delta_{11}(\hat{x}) + t_2(t_2U - t_1J)\Delta_{22}(\hat{x})\Big] \\
&\quad + 16\cos k_x \cos k_y\Big[(\frac{t_3^2}{U+J} + \frac{t_4^2}{U-J})\Delta_{11}(\hat{x}+\hat{y}) - \frac{2t_3t_4U}{U^2-J^2}\Delta_{12}(\hat{x}+\hat{y})\Big] \\
V^3(\mathbf{k}) &= \frac{4(\cos k_x - \cos k_y)}{U^2 - J^2}\Big[t_1(t_1U + t_2J)\Delta_{11}(\hat{x}) - t_2(t_2U + t_1J)\Delta_{22}(\hat{x})\Big] \\
V^1(\mathbf{k}) &= -16\sin k_x \sin k_y\Big[(\frac{t_4^2}{U+J} + \frac{t_3^2}{U-J})\Delta_{12}(\hat{x}+\hat{y}) - \frac{2t_3t_4U}{U^2-J^2}\Delta_{11}(\hat{x}+\hat{y})\Big]
\end{aligned}$$

For B1g symmetry:

$$\begin{aligned}
V^0(\mathbf{k}) &= \frac{4(\cos k_x - \cos k_y)}{U^2 - J^2}\Big[t_1(t_1U - t_2J)\Delta_{11}(\hat{x}) + t_2(t_2U - t_1J)\Delta_{22}(\hat{x})\Big] \\
V^3(\mathbf{k}) &= \frac{4(\cos k_x + \cos k_y)}{U^2 - J^2}\Big[t_1(t_1U + t_2J)\Delta_{11}(\hat{x}) - t_2(t_2U + t_1J)\Delta_{22}(\hat{x})\Big] \\
&\quad + \frac{16\cos k_x \cos k_y}{U-J}\Big[t_3^2\Delta_{11}(\hat{x}+\hat{y}) + t_3t_4\Delta_{12}(\hat{x}+\hat{y})\Big] \\
V^1(\mathbf{k}) &= 0
\end{aligned}$$

Mean Field and results

$$H_{MF} = \sum_{\mathbf{k}} \hat{\psi}^{\dagger}_{\mathbf{k}} \begin{pmatrix} \xi_{\mathbf{k}} & V(\mathbf{k}) \\ V^{\dagger}(\mathbf{k}) & -\xi_{\mathbf{k}} \end{pmatrix} \hat{\psi}_{\mathbf{k}}$$

$$\hat{\psi}^{\dagger}_{\mathbf{k}} = \left(\hat{c}^{\dagger}_{\mathbf{k}+\uparrow}, \hat{c}^{\dagger}_{\mathbf{k}-\uparrow}, \hat{c}_{-\mathbf{k}+\downarrow}, \hat{c}_{-\mathbf{k}-\downarrow}\right)$$

$$V_{\alpha\beta}(\mathbf{k}) = \sum_{nmm'n';\tau} A^{m'n'}_{nm}(\vec{\tau}) \Delta^{*}_{nm}(\vec{\tau}) e^{i\mathbf{k}\cdot\vec{\tau}} u_{m'\alpha}(\mathbf{k}) u_{n'\beta}(\mathbf{k})$$

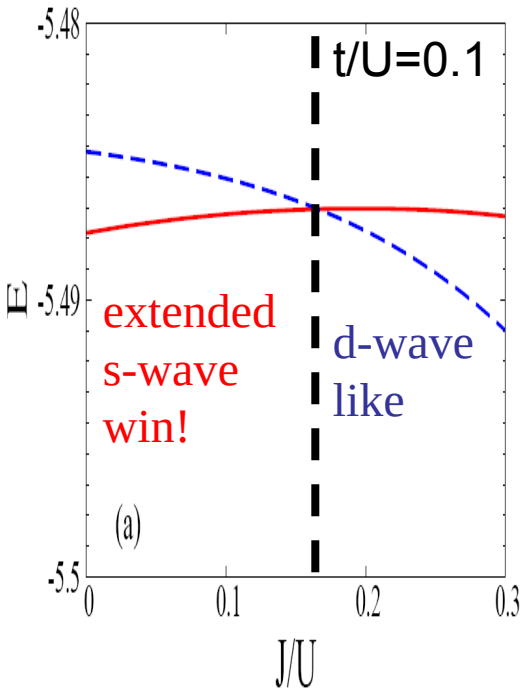

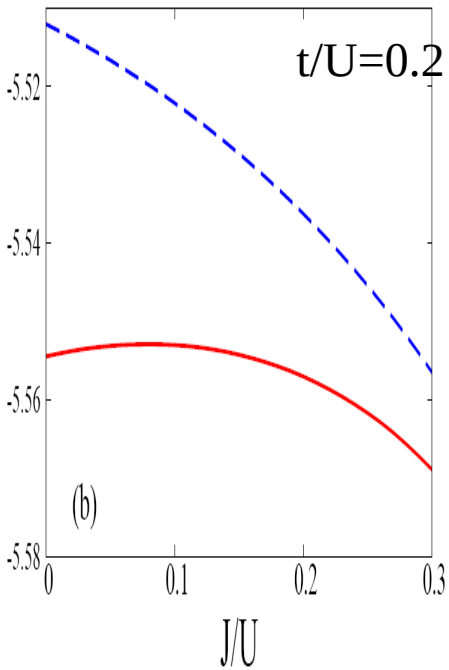

Quasiparticle gap

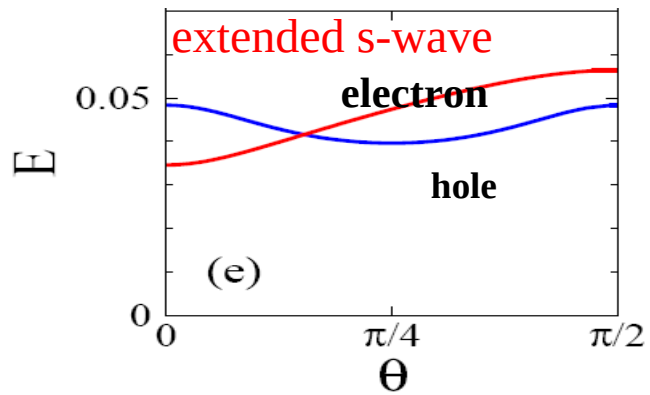

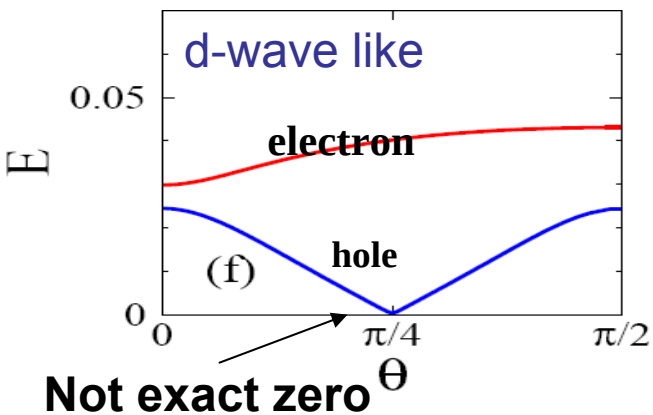

Not exact zero

Pairing amplitude distribution in momentum space – s-wave case

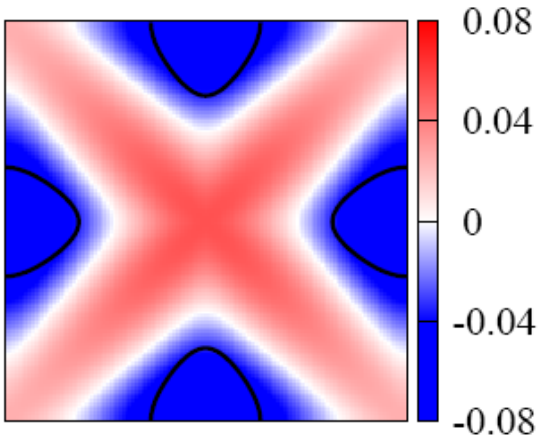

$V_{++}(k)$

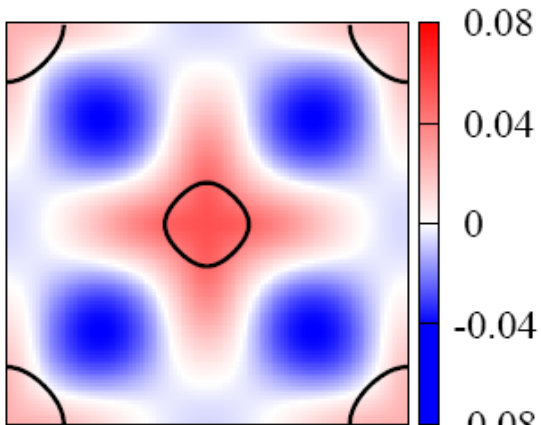

$V_{--}(k)$

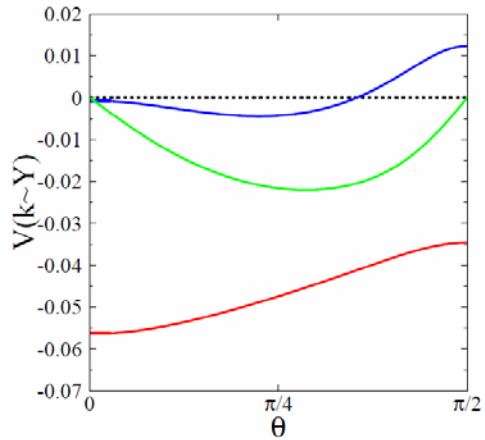

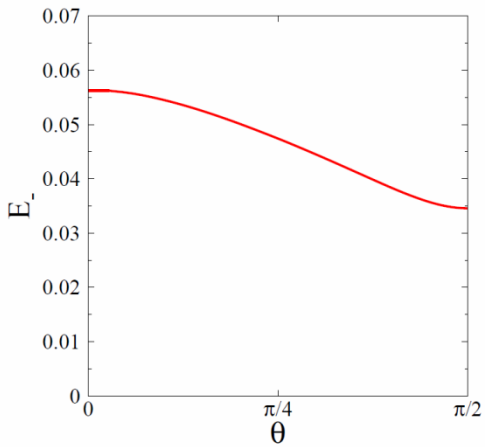

Pocket around Y
dominate by V_{++}

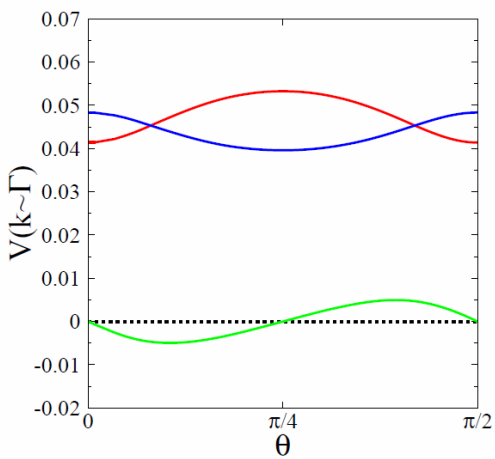

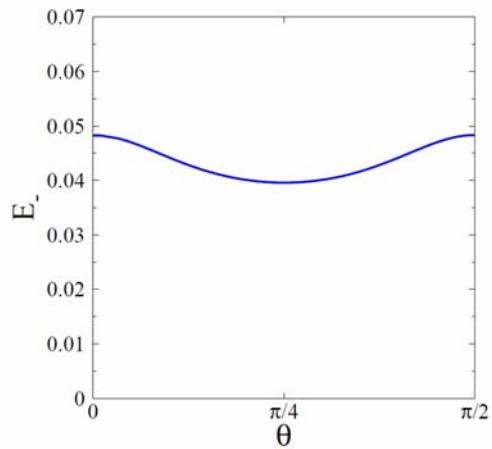

Pocket around Γ
dominate by V_{--}

Pairing amplitude distribution in momentum space – d-wave case

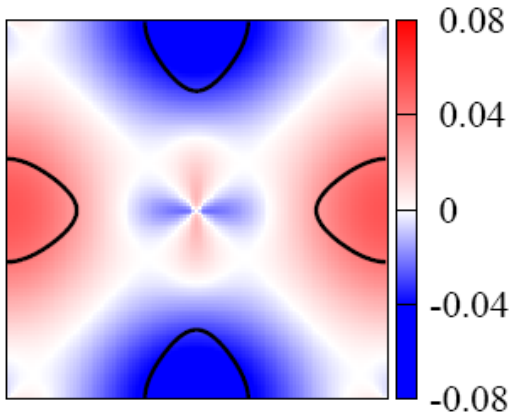

$V_{++}(k)$

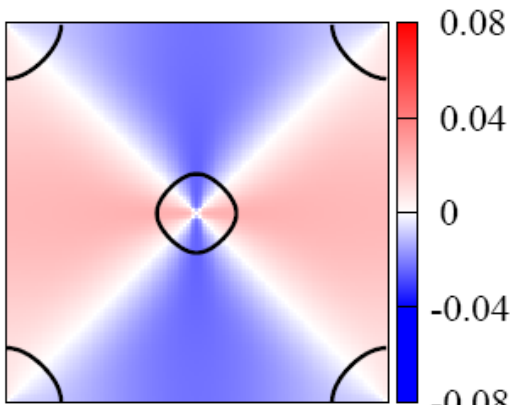

$V_{--}(k)$

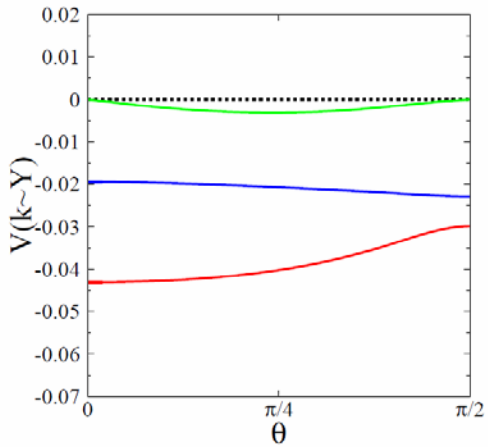

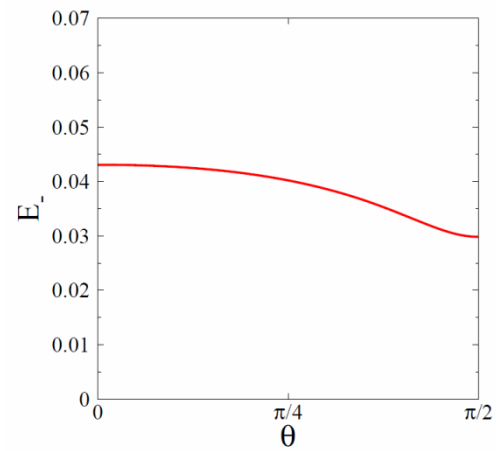

Pocket around Y
dominate by V_{++}

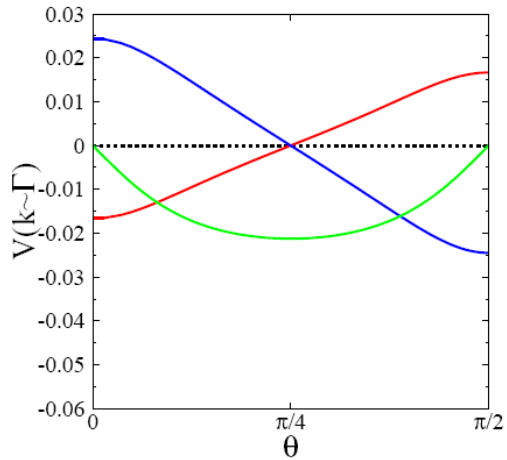

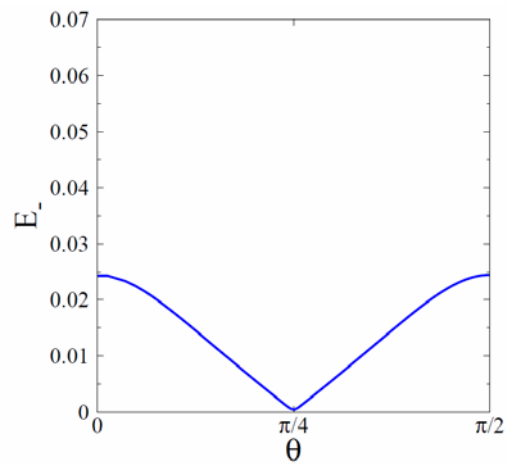

Pocket around Γ
dominate by V_{--}

Structure of pairing amplitude in momentum space

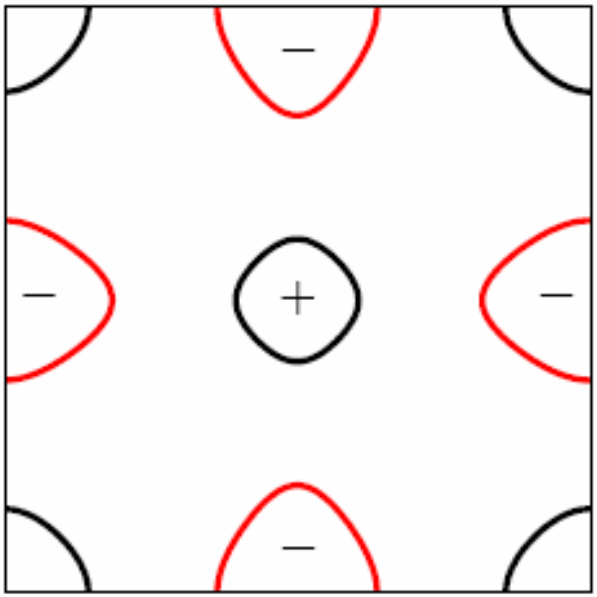

- A_{1g} symmetry
- same sign in each pocket
- different sign between hole pockets and electron pockets
- nodes does not overlap with Fermi surface
- Extended s-wave

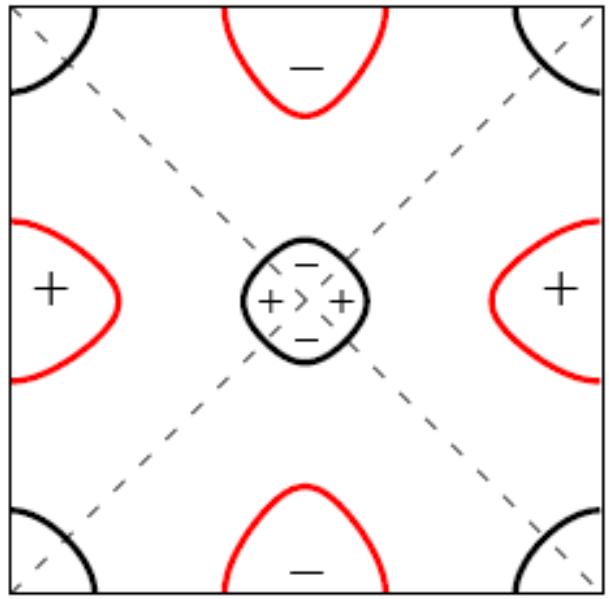

- B_{1g} symmetry
- s-wave in electron pockets
- d-wave in hole pockets
- same sign along the x axis or y axis
- d-wave like

Three orbital case

- Effective interaction

$$
\begin{aligned}
H_{\text{eff}}^{(2)} = & \sum_{i\delta}\sum_{aa'}\sum_{b\neq b'}\left[t_{\delta}^{ab}t_{-\delta}^{b'a'}\frac{2J}{U_1^2-J^2}\hat{b}_{ba}^{\dagger}(-\delta)\hat{b}_{a'b'}(\delta) - t_{\delta}^{ab}t_{-\delta}^{ba'}\frac{1}{U_2+J}\hat{b}_{b'a}^{\dagger}(-\delta)\hat{b}_{a'b'}(\delta) - t_{\delta}^{ab}t_{-\delta}^{b'a'}\frac{1}{U_2+J}\hat{b}_{b'a}^{\dagger}(-\delta)\hat{b}_{a'b}(\delta)\right] \\
& - \sum_{i\delta}\sum_{aa'}\sum_{b} t_{\delta}^{ab}t_{-\delta}^{ba'}\frac{4U_1}{U_1^2-J^2}\hat{b}_{ba}^{\dagger}(-\delta)\hat{b}_{a'b}(\delta) \\
& + \sum_{i\delta}\sum_{aa'}\sum_{b\neq b'}\sum_{s}\frac{1}{U_2-J}\left[t_{\delta}^{ab}t_{-\delta}^{ba'}\hat{T}_{b'a}^{s\dagger}(-\delta)\hat{T}_{a'b'}^{s}(\delta) - t_{\delta}^{ab}t_{-\delta}^{b'a'}\hat{T}_{b'a}^{s\dagger}(-\delta)\hat{T}_{a'b}^{s}(\delta)\right] \qquad (78) \\
= & \sum_{\mathbf{k}\mathbf{k}'}\sum_{aa'bb'} V_{a'b'}^{ab}(\mathbf{k}-\mathbf{k}')\hat{b}_{\mathbf{k}}^{ab\dagger}\hat{b}_{\mathbf{k}'}^{a'b'},
\end{aligned}
$$

- Orbital analysis (small J only)

Intra-pocket: $V < 0$

Γ to X: $V_{yz,yz}^{yz,yz} > 0 \quad V_{yz,yz}^{xz,xz} > 0 \quad V_{aa}^{xy,xy} \sim 0$

X to Y: $V_{yz,yz}^{xz,xz} < 0 \quad V_{aa}^{xy,xy} \sim 0$

Similar with 2-orbital model!

Conclusion

- We proposed a strong coupling Hamiltonian for the Fe-based superconductors derived from two-orbital Hubbard model.
- An extended s-wave pairing is found most stable in a large parameter space, consistent with ARPES experiment. But d-wave is also possible
- Orbital-dependent pairing arises from the doped charge carriers.
- Our approach may be of relevance to the intermediate coupling region, more appropriate for iron pnictides.

Iron pnictide and copper oxides

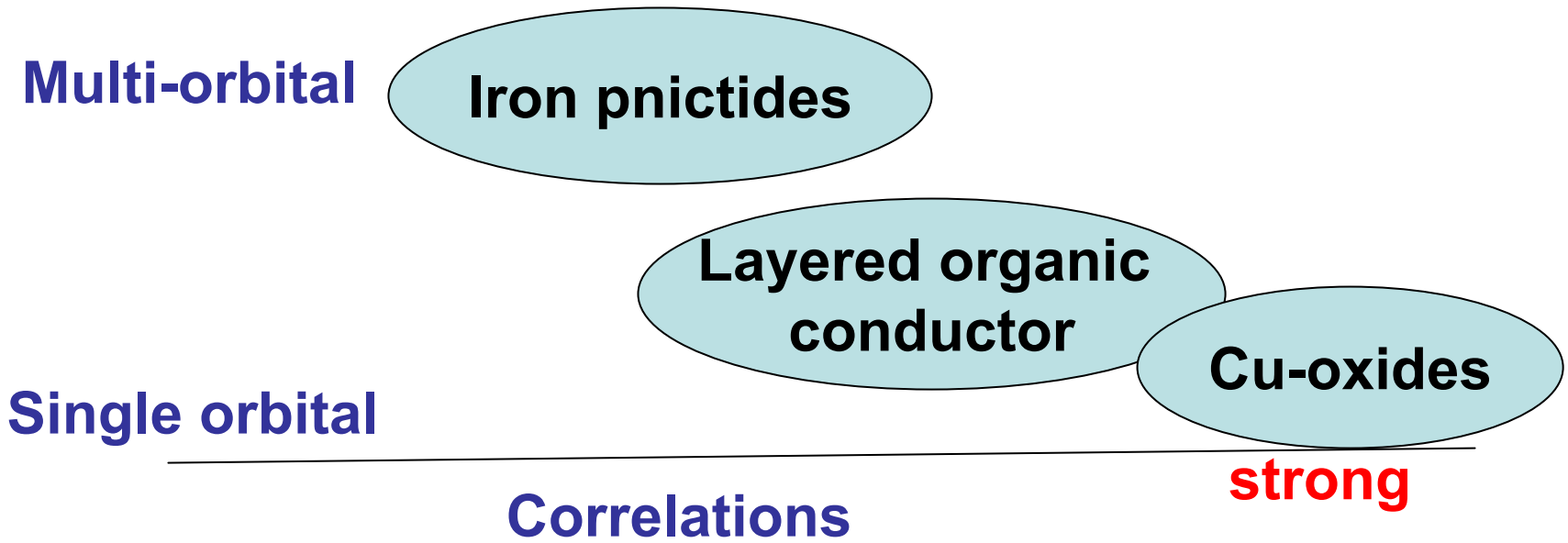

Probe anti-phase s-wave

- Symmetry is s-wave
- Phase change in magnitude of k, more difficult to probe
- Many expt. and proposed theories to probe anti-phase s-wave, seemingly one of important issue to the symmetry
- Phase sensitive expt. would provide a direct evidence

Phase sensitive expt. in LaFeAsOF, Tsuei

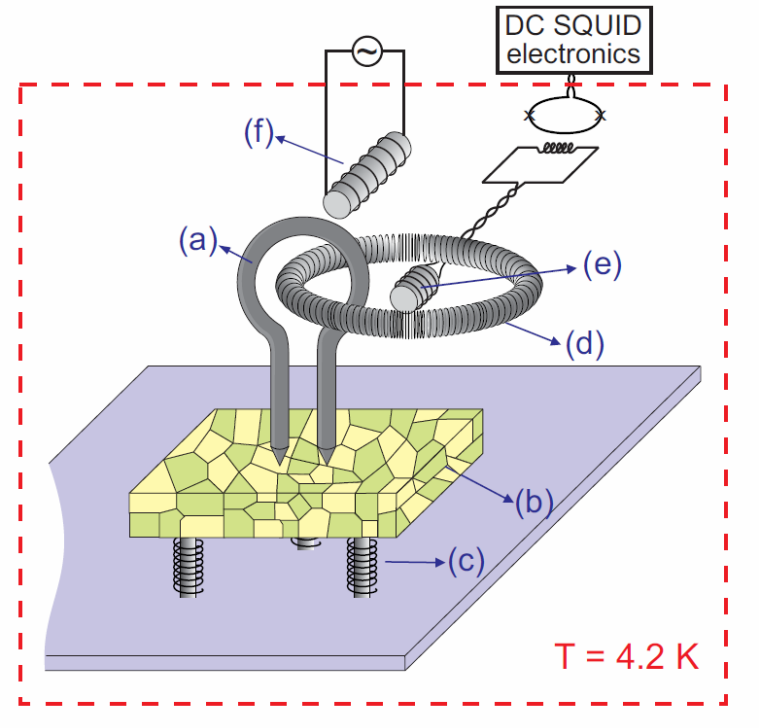

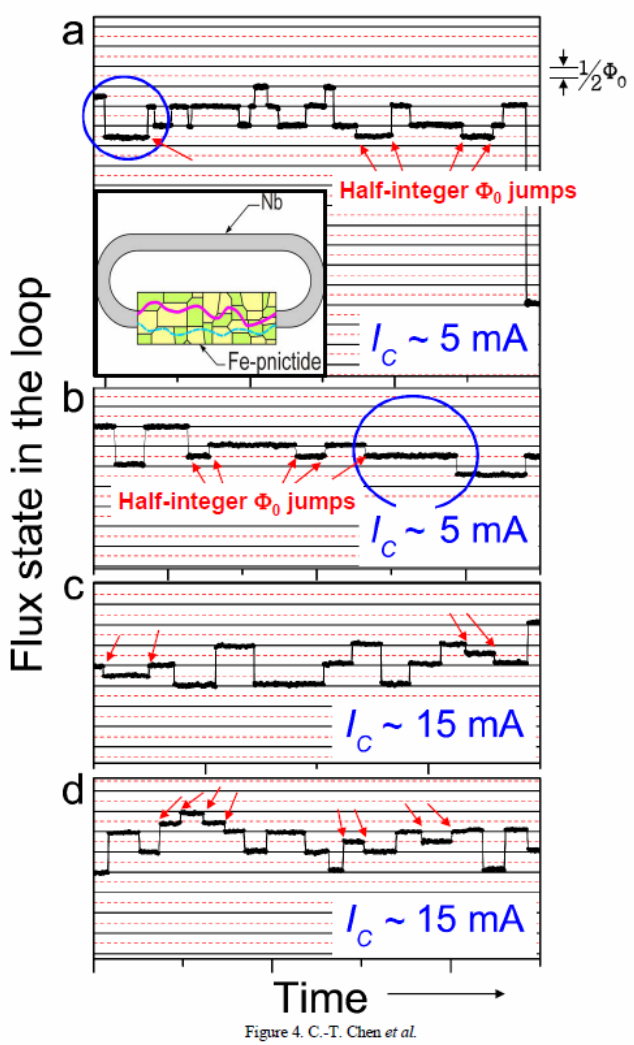

Figure 4. C.-T. Chen *et al.*

- Polycrystalline $NdFeAsO_{0.88}F_{0.12}$
- π-flux in the loop has been observed
- Effect of grain boundaries is still unclear

C.-T. Chen et al. arXiv: 0905.3571

Proposed \pi-junction loop expt.

Point contact junction

- The junction between FeAs (index 1) and a conventional SC (index 2)

$$I_c \propto \sum_\alpha \Delta_1^\alpha \Delta_2 N_{1F}^\alpha N_{2F} \int d\epsilon_1 d\epsilon_2 \; \frac{1}{E_1^\alpha E_2 [E_1^\alpha + E_2]},$$

alpha: Band index

- Because $|\Delta_2| \ll |\Delta_1^\alpha|$ according to Ambegaokar and Baratoff:

$$I_c \propto N_{2F}\Delta_2 \sum_\alpha \mathrm{sgn}(\Delta_1^\alpha) N_{1F}^\alpha K[\sqrt{1 - \frac{\Delta_2^2}{(\Delta_1^\alpha)^2}}]$$

$$\sim N_{2F}\Delta_2 \sum_\alpha \mathrm{sgn}(\Delta_1^\alpha) N_{1F}^\alpha \ln \left| \frac{4\Delta_1^\alpha}{\Delta_2} \right|,$$

$$\propto \sum_{\alpha \in BZ} \mathrm{sgn}(\Delta_1^\alpha) N_{1F}^\alpha. \quad = N_h - N_e$$

Hole density of state – electron density of states at Fermi surface

Point contact junction

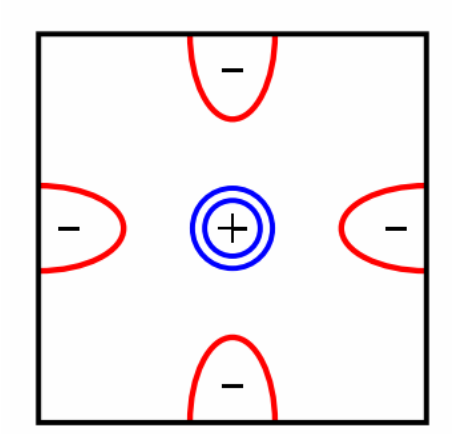

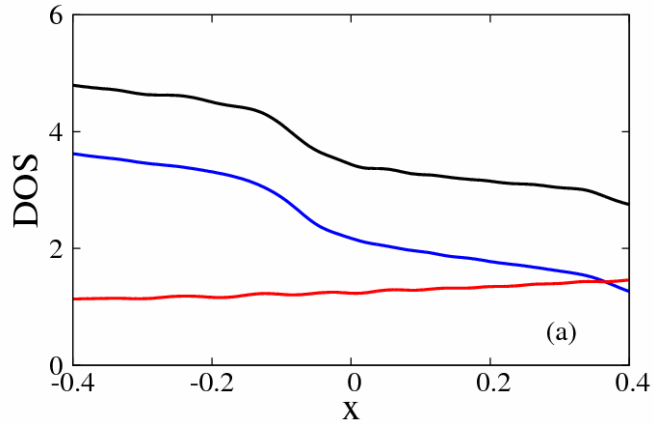

$N_h > N_e$ ⇒ 0-junction

$N_h < N_e$ ⇒ π-junction

Two e-pockets contribute to I_c

DOS of doped $BaFe_2As_2$, DFT result

blue – DOS of h-pockets (N_h)

red – DOS of e-pockets (N_e)

0-junction in most doping regime

Chen, FCZ et al. arXiv: 0906.0169

Planar junction between Al and ¯eAs

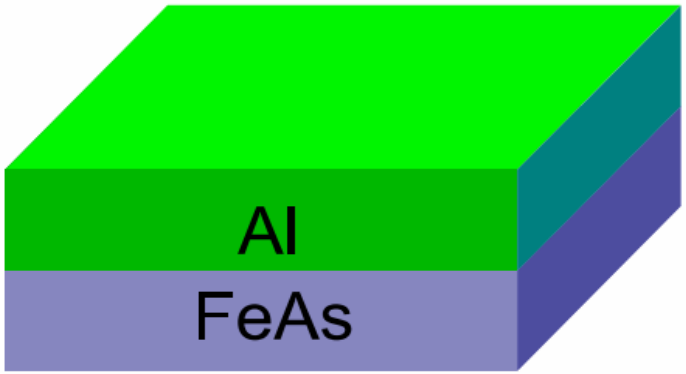

(a)

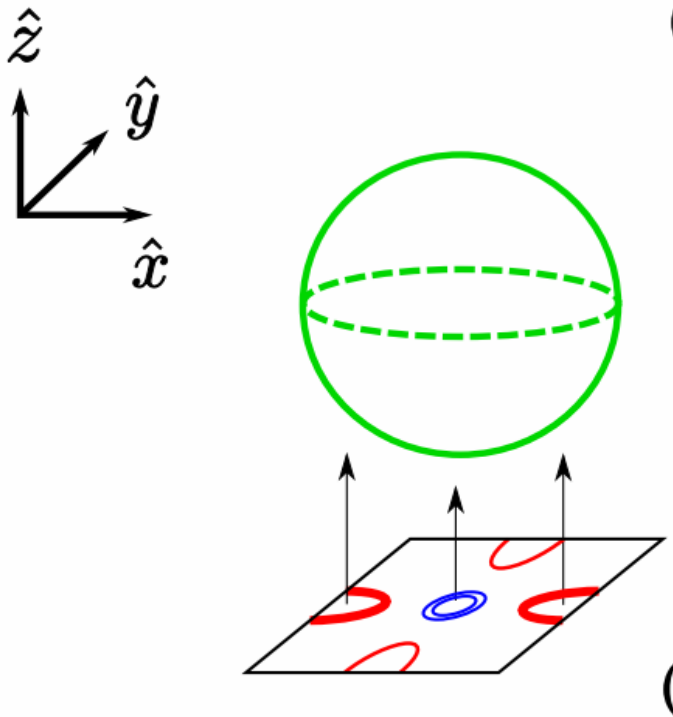

(b)

Al is a nearly free electron metal

Lattice potential is weak

Planar translation invariant.

$$T_{\mathbf{kq}} = T_0 \delta_{k_{xy}, q_{xy}}$$

Chen, FCZ et al. arXiv: 0906.0169

Planar junction between Al and FeAs

$$I_c \propto T_0^2 \Delta_2 \sum_{\alpha \in q_F} \Delta_1^\alpha \int d\mathbf{k} dq_z \frac{1}{E_1^\alpha(\mathbf{k}) E_2(k_{xy}, q_z)[E_1^\alpha(\mathbf{k}) + E_2(k_{xy}, q_z)]}$$

$$\propto \sum_\alpha \frac{\mathrm{sgn}(\Delta_1^\alpha) N_{1F}^\alpha}{\sqrt{q_F^2 - Q_\alpha^2}} \propto N_h - cN_e \begin{cases} \text{0-junction, } N_h/N_e > c \\ \text{π-junction, } N_h/N_e < c \end{cases}$$

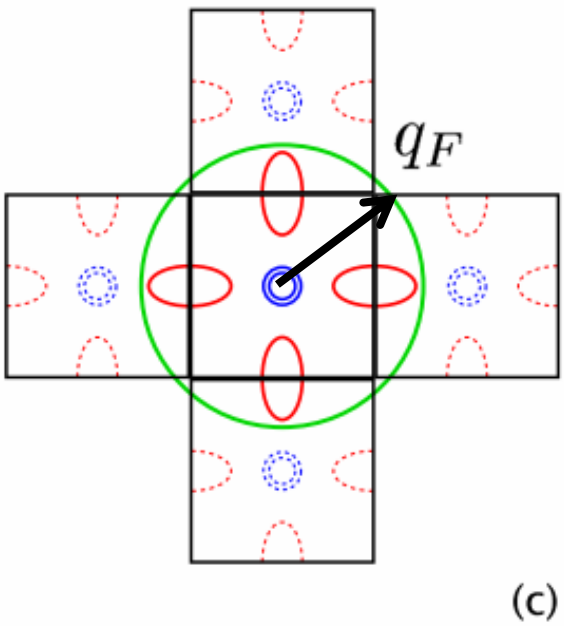

- In the vicinity of FS:

$$q \sim q_F \Rightarrow k_{xy} \lesssim q_F$$

- Four electron pockets.
- E-pockets are further enhanced by $1/\sqrt{q_F^2 - Q_\alpha}$
- c ~ 2.58

Chen et al. arXiv: 0906.0169

Proposed setup

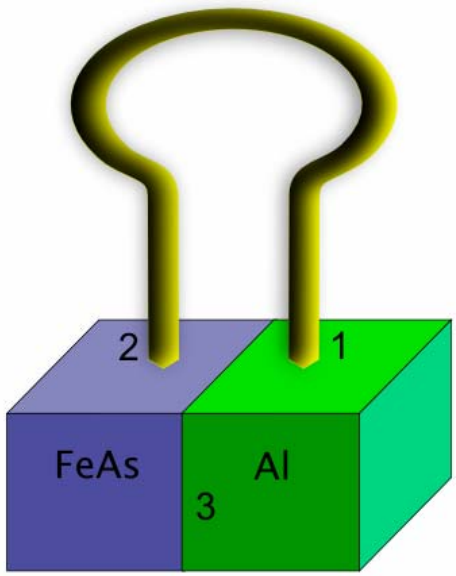

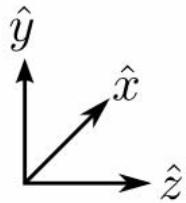

Three junctions:

1. 0-junction.
2. 0-junction for $N_h/N_e > 1$

   π-junction for $N_h/N_e < 1$
3. 0-junction for $N_h/N_e > c$

   π-junction for $N_h/N_e < c$

The condition to realize a π-junction loop

$$1 < N_h/N_e < c \sim 2.58$$

satisfied in very large doping regions.

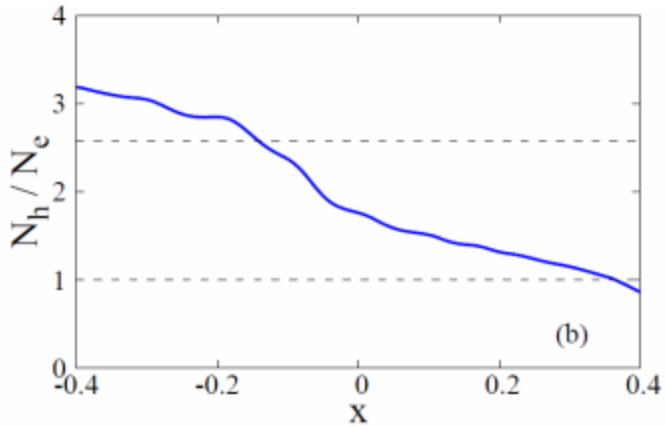

The calculation based on DFT results gives similar result!

Chen et al. arXiv: 0906.0169

Summary of \pi-junction loop

- The sign of a point-contact junction is positive if $N_h > N_e$ and is negative otherwise.

- In the planar junction between a single crystal Fe-pnictide and Al, planar translational enhances the contribution of electron pockets to the critical current.

- We have proposed a type of Josephson tri-junction to probe the $s_{\pm}$ pairing state in Fe-pnictide, which appears to be accessible in experiments.

Thanks